Laminar Displacement and Prelaminar Tissue Thickness Change after Glaucoma Surgery Imaged with Optical Coherence Tomography

Alexandre S. C. Reis,[1,2] *Neil O'Leary,*[1] *Miriam J. Stanfield,*[1] *Lesya M. Shuba*[1] *Marcelo T. Nicolela,*[1] *and Balwantray C. Chauhan*[1]

Purpose. To study changes in lamina cribrosa position and prelaminar tissue thickness (PTT) after surgical IOP reduction in glaucoma patients.

Methods. Twenty-two patients (mean age, 71.4 years) were imaged with spectral domain optical coherence tomography (SD-OCT; 24 radial B-scans centered on the optic nerve head [ONH]) before trabeculectomy or tube shunt implantation. Follow up images were acquired 1 week, 1 month, 3 months, and 6 months postsurgery. Bruch's membrane opening (BMO), the internal limiting membrane (ILM) and the anterior laminar surface (ALS) were segmented in each radial scan with custom software. Surfaces were fitted to the ILM and ALS with the extracted three-dimesional coordinates. PTT was the distance between the ILM and ALS, perpendicular to a BMO reference plane. Serial postsurgical laminar displacement (LD), relative to the BMO reference plane, and changes in PTT were measured. Positive values indicated anterior LD.

Results. Mean (SD) presurgery IOP was 18.1 (6.5) mm Hg, and reduced by 4.7 (5.5), 2.4 (7.7), 7.0 (6.2), and 6.8 (7.5) mm Hg at 1 week, 1 month, 3 months, and 6 months postsurgery, respectively. At the four postsurgery time points, there was significant anterior LD (1.8 [9.5], −1.1 [8.9], 8.8 [20.2], and 17.9 [25.8] μm) and PTT increase (1.7 [13.3], 2.4 [11.9], 17.4 [13.7], and 13.9 [18.6] μm). LD was greater in ONHs with larger BMO area ($P = 0.01$) and deeper ALS ($P = 0.04$); however, PTT was not associated with any of the tested independent variables.

Conclusions. Both anterior LD and thickening of prelaminar tissue occur after surgical IOP reduction in patients with glaucoma. (*Invest Ophthalmol Vis Sci.* 2012;53:5819–5826) DOI:10.1167/iovs.12-9924

Biomechanical factors acting within the optic nerve head (ONH), particularly at the level of the lamina cribrosa, likely play a role in retinal ganglion cell (RGC) axonal loss in glaucoma.[1,2] The lamina is the key structure around which obstruction of axoplasmic transport has been noted by various investigators in experimental models of glaucoma.[3–5] While the precise mechanisms of axoplasmic transport obstruction are not fully understood, they could be related to the significant pressure gradient RGC axons experience as they pass through the lamina from intraocular to retrolaminar tissue space,[6] or to the connective tissue changes that occur with disease progression.[1,7] Considerable research has centered on the biomechanical changes in the ONH, specifically in and around the lamina, and how they may help explain the pathophysiology of glaucoma.[7] One approach in this research is determining how the lamina and prelaminar tissues respond to IOP change.

Reversal of optic disc cupping after successful glaucoma surgery is observed commonly in children[8,9] and to a lesser extent in adults.[10,11] Several studies have examined ONH surface changes with confocal scanning laser tomography (CSLT) after surgical[12–17] or medical[18,19] reduction of IOP. However, because CSLT is able to image only ONH surface changes, none of these earlier studies were able to evaluate the contribution of deep ONH structures resulting in the increase of neuroretinal rim area and decrease of optic disc cupping after IOP reduction. With spectral domain optical coherence tomography (SD-OCT),[20,21] and enhanced depth imaging (EDI),[22] it is now possible to visualize the anterior laminar surface (ALS) in vivo, and in more recent reports even the posterior laminar surface.[23–26]

We recently showed that ONH surface changes due to acute IOP elevation represent mostly compression of prelaminar tissue and not posterior laminar displacement (LD).[27] The present study was conducted to determine whether the anterior movement of the ONH surface after reduction in IOP is caused primarily by changes in the prelaminar tissues or in laminar position. The objectives of this study were (1) to evaluate LD and prelaminar tissue thickness (PTT) changes in glaucoma patients undergoing surgical IOP reduction, and (2) to determine whether factors such as age, IOP, and presurgery PTT were associated with LD and PTT changes.

Methods

Patients

Twenty-two patients with open-angle glaucoma from the Queen Elizabeth II Health Sciences Centre in Halifax, Nova Scotia were enrolled in this prospective observational study. Patients were scheduled for glaucoma surgery in the referral practices of two of the authors (LMS and MTN) and underwent SD-OCT imaging pre- and postsurgery. The research adhered to the tenets of the Declaration of Helsinki and subjects gave informed consent to participate in the study.

From the [1]Department of Ophthalmology and Visual Sciences, Dalhousie University, Halifax, Nova Scotia, Canada; and the [2]Department of Ophthalmology, University of Sao Paulo, Sao Paulo, Brazil.

Submitted for publication March 27, 2012; revised June 13, 2012; accepted July 13, 2012.

Disclosure: **A.S.C. Reis**, None; **N. O'Leary**, None; **M.J. Stanfield**, None; **L.M. Shuba**, None; **M.T. Nicolela**, None; **B.C. Chauhan**, Heidelberg Engineering GmbH (F, R, S)

Corresponding author: Balwantray C. Chauhan, Department of Ophthalmology and Visual Sciences, Dalhousie University, 1276 South Park Street, 2W Victoria, Halifax, Nova Scotia, Canada B3H 2Y9; bal@dal.ca.

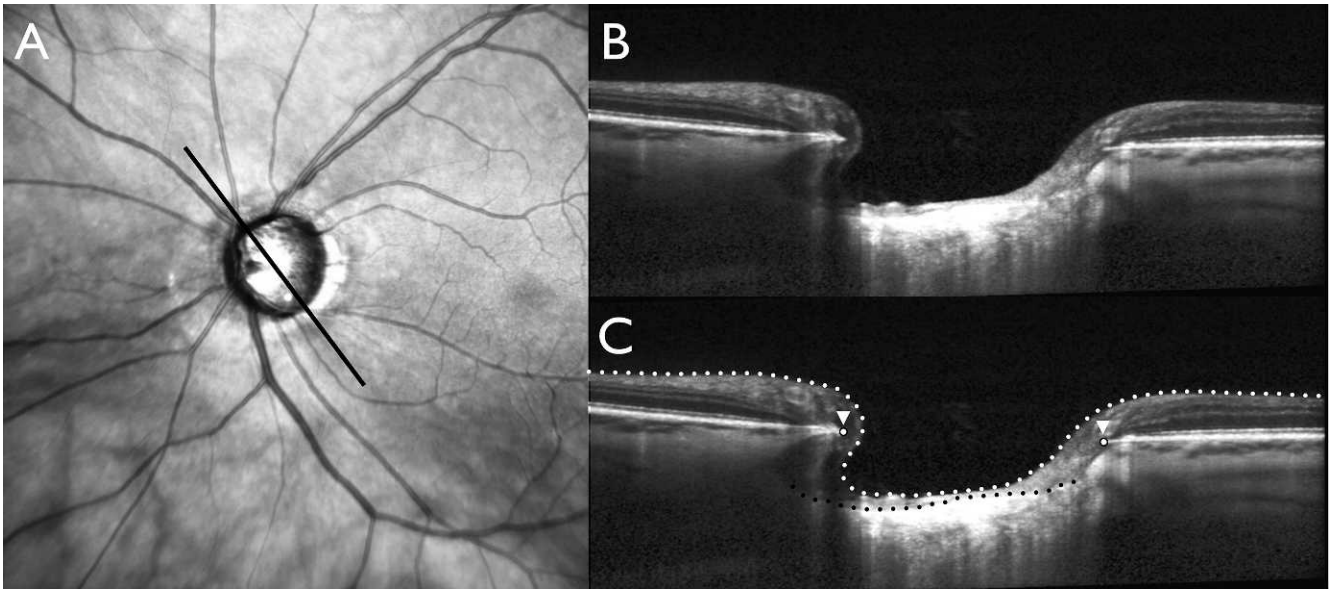

Figure 1. Segmentation of the optic nerve head structures. Infrared image (**A**) shows the radial section where the B-scan (**B**) was acquired. (**C**) B-scan with the segmented structures: (1) internal limiting membrane (*white dotted line*), (2) anterior laminar surface (*black dotted line*), and (3) Bruch's membrane opening (*white dots indicated by white arrowheads*).

The protocol was approved by the Capital Health Research Ethics Board.

Inclusion criteria were (1) a clinical diagnosis of open-angle glaucoma with documented progressive optic disc change and/or visual field damage compatible with glaucoma, (2) best corrected visual acuity equal to or better than 0.3 (20/40) logarithm minimum angle of resolution in the study eye, and (3) refraction within ±6.00 diopters (D) sphere and ±3.00 D astigmatism. Exclusion criteria were (1) concomitant ocular disease, and (2) systemic medication known to affect the visual field. Only one eye of each patient was included in this study.

The glaucoma surgical procedures were either trabeculectomy or tube shunt implantation. Surgery was performed when there was one or both of the following indications: (1) documented and confirmed visual field and/or optic disc progression, and (2) IOP considered clinically too high for the level of glaucomatous damage. Suture lysis, bleb needling revision, 5-fluorouracil subconjunctival injection, and topical ocular hypotensive medications were used at the discretion of the treating surgeon postoperatively, as clinically indicated.

Imaging

Each subject had the study eye imaged through undilated pupils with a commercially available SD-OCT device (Spectralis; Heidelberg Engineering GmbH, Heidelberg, Germany) prior to surgery. The presurgery image was acquired on the same day, or at most, one week prior to surgery. Follow up postsurgery images were acquired at 1 week, 1 month, 3 months, and 6 months after surgery at the same locations as the presurgery image with the internal registration software. A radial scanning pattern centered on the ONH was used (24 high resolution 15° radial scans, each averaged from 30 B-scans with 768 A-scans per B-scan acquired with scanning speed of 40,000 A-scans per second). Subjects were imaged using the EDI technique described in detail elsewhere.[22] In brief, because the infrared center wavelength (870 nm) of the light source results in a relatively lower signal-to-noise ratio for deeper ONH structures when focused on internal limiting membrane (ILM), the focus is shifted to deeper locations to allow enhanced imaging of deeper structures such as the lamina.

Segmentation of ONH Structures in SD-OCT Images

SD-OCT raw data were imported into customized software based on the Visualization Toolkit (VTK, Clifton Park, NY),[28,29] enabling three-dimensional (3D) visualization and manual segmentation of SD-OCT structures. Within each radial B-scan one author (ASCR) manually segmented the ILM and the ALS, defined as the highly reflective region beneath the ILM. Bruch's membrane opening (BMO), defined as the termination of the retinal pigment epithelium/Bruch's membrane complex (one point on each side of the B-scan) was also segmented. Figure 1 illustrates a manually segmented B-scan.

Data Analysis

The segmentation of the 24 radial B-scans yielded a 3D point cloud describing the ILM, the ALS, and BMO. Surfaces were fitted to the ILM and ALS with the extracted 3D coordinates. A spline was fitted to the BMO points around the ONH to generate a closed curve within which the BMO area was computed. In addition, a best-fit plane representing the BMO points was derived creating a BMO reference plane (Fig. 2). Laminar position measurements in pre- and postsurgery images were made relative to the BMO reference plane.

For each time point, PTT was defined as the mean perpendicular distance (direction normal to the BMO reference plane) between the overlapping en face segmented ILM surface and ALS. The mean perpendicular distance from the BMO reference plane to the ALS, measured within BMO, was termed the ALS height. The LD resulting from IOP change was computed as the mean difference between post- and presurgery ALS heights, with positive values indicating anterior displacement and negative values indicating posterior displacement. The PTT change resulting from IOP change was computed as the difference between post- and presurgery PTT. In order to compute and compare serial LD and PTT changes, only data from the overlapping en face segmented ILM surface and ALS inside BMO in the pre- and postsurgery images (i.e., those locations with common valid values at the x and y coordinates throughout the follow up) were analyzed.

Repeated measures ANOVA was used to evaluate changes in IOP and ONH parameters following surgery. Spearman's rank correlation coefficient ρ was used to test the relationship between LD and PTT change, and their relationship with IOP. Multiple regression analysis

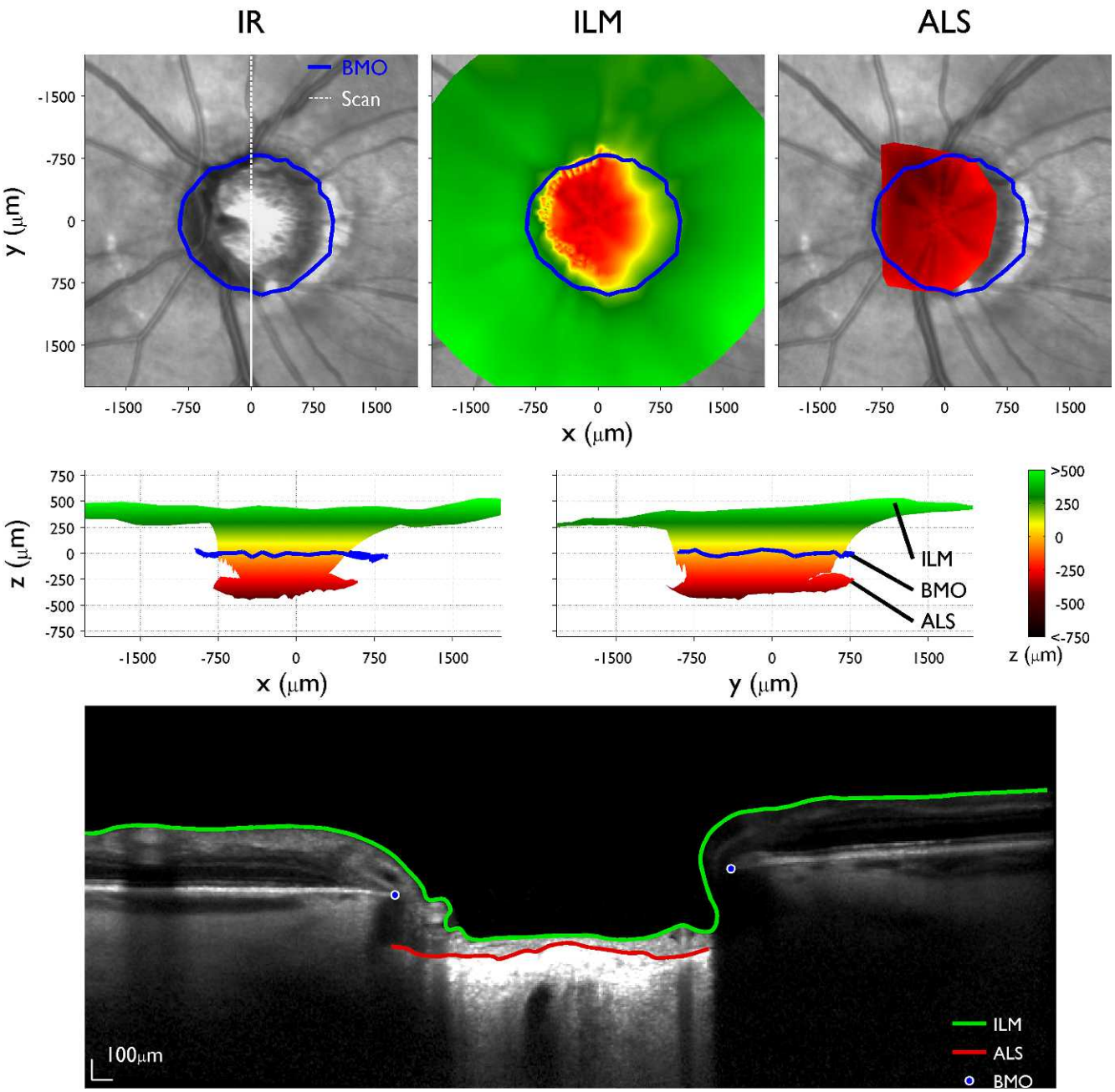

Figure 2. Graphical representation of optic nerve head surfaces derived from manual segmentation from the left eye of a study patient. The top panel shows (1) the infrared (IR) image, on which the *blue line* represents the BMO projected from the segmented BMO positions in the B-scans. The *white dashed line* indicates the location where the scan shown in the bottom panel was acquired, (2) the ILM surface in en face view, and (3) the ALS in en face view. The middle panel shows the ILM and ALS surfaces, and BMO along the horizontal (*left*) and vertical (*right*) axes. The heights (*z*-axis) are color coded according to the legend. The bottom panel shows the scan indicated in the IR image with the manual segmentation of the ILM, ALS, and BMO.

Table 1. Intraocular Pressure Characteristics Pre- and Postsurgery*

		Postsurgery			
	Presurgery	**1 Wk**	**1 Mo**	**3 Mos**	**6 Mos**
IOP†	18.1 (6.5)	13.6 (6.1)	15.6 (10.3)	11.3 (4.3)	11.4 (5.3)
Absolute IOP reduction		4.7 (5.5)	2.4 (7.7)	7.0 (6.2)	6.8 (7.5)
% IOP reduction		22.8 (31.3)	14.9 (44.1)	35.8 (21.6)	33.9 (29.3)

* Values shown are mean (SD) in millimeter of mercury unless otherwise indicated.
† $P < 0.05$ repeated measures ANOVA.

Table 2. Laminar Displacement and Prelaminar Tissue Thickness Characteristics*

		Postsurgery			
	Presurgery	**1 Wk**	**1 Mo**	**3 Mos**	**6 Mos**
LD		1.8 (9.5)	−1.1 (8.9)	8.8 (20.2)	17.9 (25.8)
PTT	232.0 (117.4)	227.9 (124.8)	203.8 (99.3)	235.9 (109.7)	245.9 (117.7)
PTT change		1.7 (13.3)	2.4 (11.9)	17.4 (13.7)	13.9 (18.6)

* Values shown are mean (SD) in micrometers.

was performed to establish whether the independent variables of age, presurgery IOP, ALS height, PTT and BMO area, and mean postsurgery IOP were associated with the mean postsurgery LD and PTT change. Analyses were carried out with Matlab (MathWorks, Natick, MA) and SPSS Statistics v. 19 (IBM SPSS Statistics, Armonk, NY).

Results

There were 13 (60%) men and 9 (40%) women of European ancestry in the study. The mean (range) age was 71.4 (47.0–88.2) years and the visual field mean deviation, –9.5 (–2.4 to –18.8) dB. Eighteen (81%) patients underwent trabeculectomy and four (19%) tube shunt implantation. None of the 22 patients had IOP less than 5 mm Hg at any time during the follow up, gross macular or optic disc edema after surgery, major surgical complications, or required additional surgery during the follow up period. There was a statistically significant IOP reduction over 6 months of follow up (Table 1, $P < 0.01$). The mean (SD) value of the mean absolute deviation of the BMO points from the fitted BMO reference plane was 15.4 (6.0) μm.

The mean (SD) BMO area was 1.81 (0.42) mm^2 presurgery, and was not statistically different postsurgery: 1.79 (0.39) mm^2, 1.83 (0.38) mm^2, 1.84 (0.43) mm^2, and 1.81 (0.41) mm^2, at 1 week, 1 month, 3 months, and 6 months, respectively ($P = 0.30$). The ALS area segmented in the study was on average 57 (18%) of the BMO area, and the overlap in the segmented en face ALS in the pre- and postsurgery images was 47 (16%).

The mean presurgery PTT was 232.0 μm, and increased significantly by 1.7 to 17.4 μm in the postsurgery follow up ($P = 0.02$; Table 2 and Fig. 3). Additionally, postsurgery, the ALS displaced anteriorly with mean LD of 1.8 to 17.9 μm ($P < 0.01$; Table 2 and Fig. 3). There was no difference between LD and PTT change at any of the postsurgery time points ($P > 0.12$) and generally a weak negative correlation between these two variables (ρ from –0.19 to –0.56, Fig. 4).

In multivariate regression analyses, LD was positively associated with baseline BMO area ($P = 0.01$; Table 3) and negatively associated with baseline ALS height. PTT change was not associated with any of the studied variables (Table 3). The models for LD and PTT yielded adjusted R^2 values of 0.46 ($P = 0.01$), and –0.13 ($P = 0.75$), respectively.

A representative case example of a 62-year-old patient with anterior LD and PTT change is shown in Figure 5. The presurgery IOP was 14 mm Hg and the postsurgery IOP was 9, 6, 5, and 8 mm Hg at 1 week, 1 month, 3 months, and 6 months, respectively. The LD and PTT change for this patient are indicated in Figure 4.

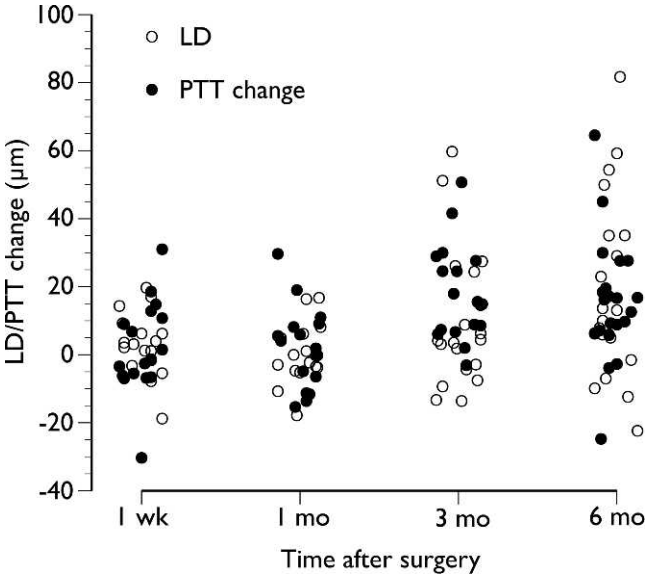

Figure 3. Laminar displacement (LD) and prelaminar tissue thickness (PTT) change at the four postsurgery time points (1 week, 1 month, 3 months, and 6 months). Data points represent observations in individual patients jittered along the *x*-axis for better visualization. wk, week; mo, month(s).

Discussion

Anterior displacement of the ONH surface resulting from acute reduction in IOP has been observed in adult glaucoma patients undergoing trabeculectomy[12–17] and in a subset of patients with a large IOP reduction after medical treatment.[18,19] Because these studies used CSLT in which the ALS cannot be visualized, the source of ONH surface changes cannot be precisely elucidated. Backward bowing of the lamina has long been recognized as a characteristic feature of glaucomatous optic neuropathy.[30–32] It can be speculated that with postsurgical IOP reduction, anterior repositioning of the posteriorly displaced lamina and partial filling in of the optic disc cup occurs.[11] The advent of SD-OCT has made it possible to image the ALS in the presence of overlying prelaminar tissue and to quantify its displacement with IOP change.[27]

The main finding of this study was that with mean IOP reduction of around 7 mm Hg at 3 and 6 months postsurgery, there was both prelaminar tissue thickening and anterior laminar displacement. On average PTT increased by 17 and 14 μm at 3 and 6 months postsurgery, respectively, while the corresponding average anterior LD was 9 and 18 μm.

Previous investigators hypothesized that anterior ONH surface changes after IOP reduction could be due to anterior movement of the lamina cribrosa or thickening of prelaminar tissue.[10,11,33] Our results support both these hypotheses, and indicate that anterior displacement of the lamina cribrosa alone cannot fully explain ONH surface changes. Prelaminar tissue thickening can occur due to an increase in blood volume with associated changes in blood flow,[34] or a shift of axoplasmic fluid from both the peripapillary retinal nerve fiber layer into prelaminar tissue and fluid that had been pushed

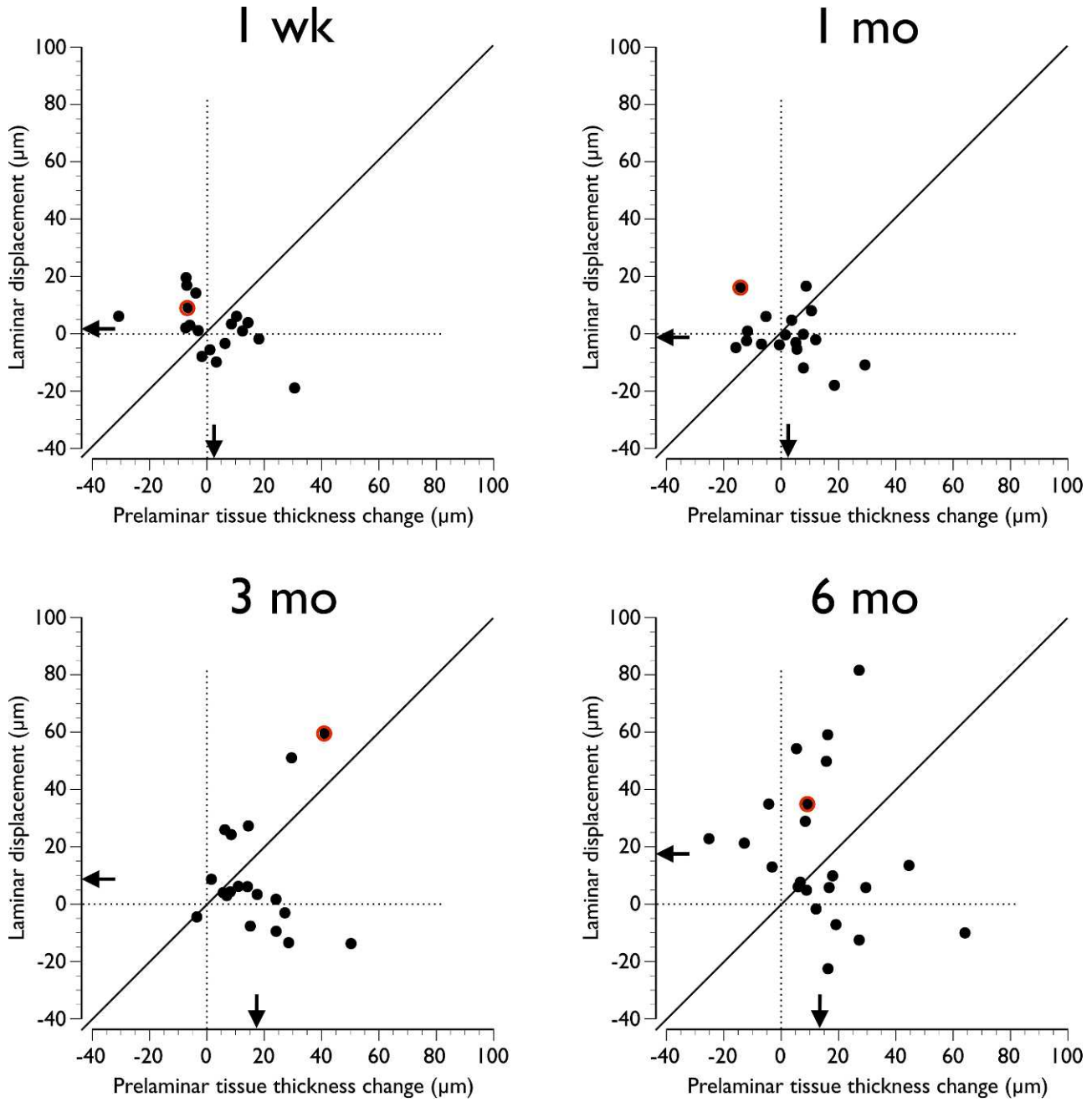

Figure 4. Laminar displacement (LD) as a function of the prelaminar tissue thickness (PTT) change at the four postsurgery time points (1 week, 1 month, 3 months, and 6 months). *Solid diagonal line* represents equal LD and PTT change. *Arrows* indicate mean values. *Red circles* around data points indicate values for the case report shown in Figure 5.

Table 3. Results of Multivariate Regression Analyses of Mean Postsurgery Laminar Displacement and Prelaminar Tissue Thickness Change*

	LD		PTT Change	
	Coefficient	***P***	**Coefficient**	***P***
Age	−0.36	0.12	−0.32	0.24
Presurgery IOP	−0.80	0.12	0.81	0.18
Presurgery ALS height	−0.04†	0.04	0.04	0.10
Presurgery PTT	0.01	0.68	0.00	0.93
Presurgery BMO area	15.62‡	0.01	1.80	0.78
Absolute IOP reduction	0.26	0.70	−0.74	0.37

* Values shown are unstandardized regression coefficients.

downstream through the lamina at higher IOP levels.[3,5,35] Subclinical ONH edema is also a possible explanation for ONH surface changes following IOP reduction[36]; however, since this most likely occurs in the early postoperative period, it probably does not explain the PTT changes persisting 6 months after surgery.

Previous research has demonstrated that the degree of ONH surface displacement is generally related to the degree of IOP change,[13–17] although the effects are variable[37] and may not be linear.[33,38] However, the various effects of IOP change on ONH structures described in experimental[27,33,38–40] and computer simulation[41–43] studies demonstrate that complex interactions between multiple variables are likely responsible for the observed results. Factors such as scleral[2,44] and laminar

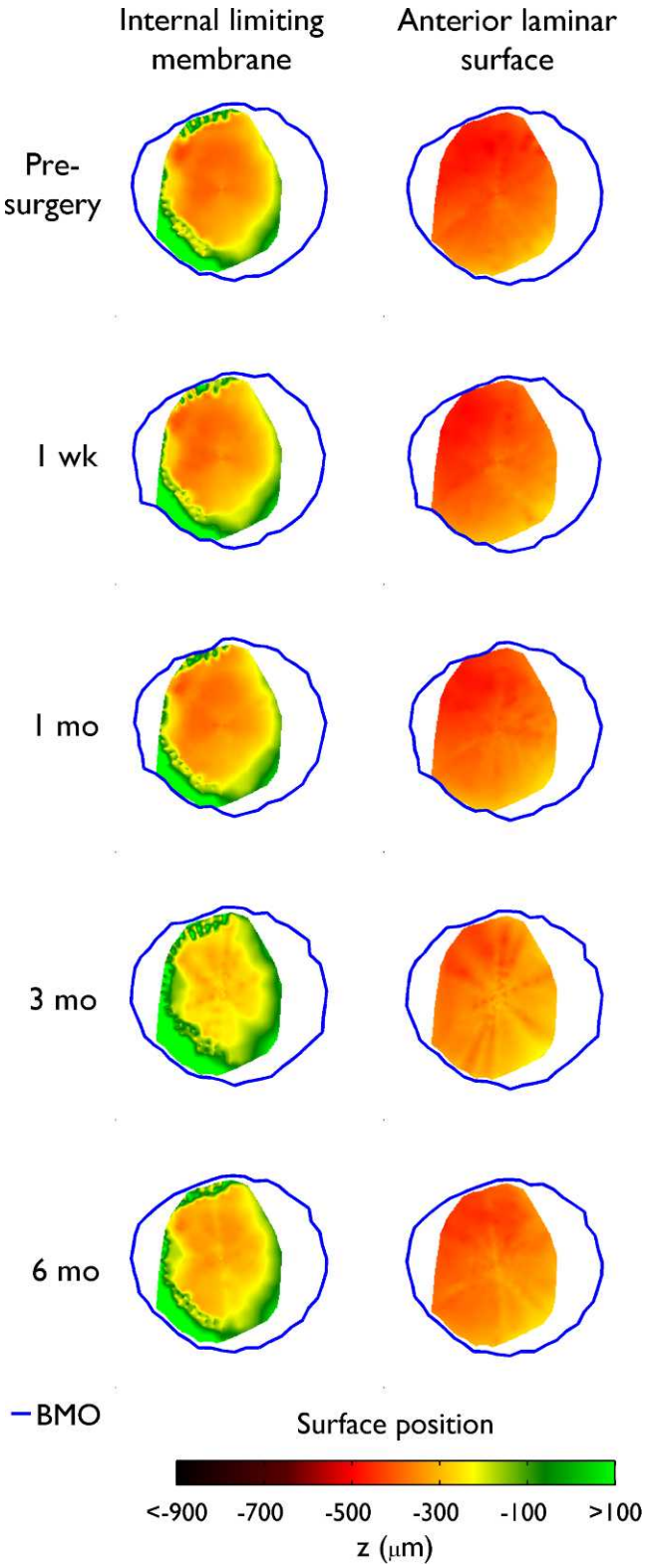

FIGURE 5. Study patient illustrating progressive forward displacement of the internal limiting membrane (*left*) and anterior laminar surface (*right*) at the four postsurgery time points (1 week, 1 month, 3 months, and 6 months). Presurgery (baseline) data are also shown. The corresponding LD and PTT change values are also shown in Figure 4.

thickness[31,45] may be important to structural compliance. Recent work from Sigal and colleagues[46] suggests that the lamina does not respond to changes in IOP in isolation, but rather that the ONH and peripapillary sclera behave as a mechanical system, and that the magnitude of the final response of ONH structures to IOP may be blunted due to interactions of other factors to maintain the ONH as a robust structure.[47]

In the present study, both LD and PTT change were more pronounced at 3 and 6 months postsurgery when there was maximal decrease in IOP. However, in multivariate regression analyses there appeared to be no statistically significant association between the degree of mean postsurgery IOP and either mean postsurgery LD or PTT change. LD was positively related to BMO area, indicating that the effects of IOP reduction on the lamina were more pronounced in ONHs with a larger neural canal opening. Additionally, there was greater anterior LD in ONHs with a deeper anterior lamina position relative to the BMO reference plane.

This study has some limitations. Because the entire ALS could not be visualized, largely because of the shadowing from the large vessels, it was not fully segmented. The LD values are reported from an average of 47% of BMO area, hence, it is possible that the lamina and prelaminar tissue in non-segmented portions could behave differently under IOP modulation compared with those that were segmented. We could not consistently visualize the posterior laminar surface, making it impossible to assess information regarding deformation of the entire lamina. Although we had highly reliable lateral anatomical registration over time, the nature of serial SD-OCT examinations necessitates a relative axial reference plane. We chose the BMO as a reference plane to derive ALS height. Although the BMO area was not altered as a result of surgical IOP reduction, we could not determine whether the BMO plane was axially stable because all measurements were made relative to it. For this reason, we also calculated the LD relative to a peripheral ILM reference plane, akin to the reference ring used in the CSLT. These analyses yielded almost identical results to those obtained with a BMO reference plane, suggesting that there were no nonuniform changes in these two reference planes. Unlike LD, changes in PTT did not depend on a reference plane as PTT was computed as the mean perpendicular distance from the ILM to the ALS. While we performed analysis at the population level, our study lacked a control group of glaucoma patients who were matched for the examined baseline characteristics followed in the same manner to gauge the reproducibility of measurements within and between sessions at the individual patient level. The relatively small sample size could have resulted in a failure to statistically confirm the significance of other factors determining LD and PTT change.

In summary, both forward anterior laminar surface displacement and prelaminar tissue thickening occur in response to IOP decrease after glaucoma surgery. The changes are persistent to at least 6 months postsurgery.

Acknowledgments

The authors thank Claude Burgoyne, MD, for providing the segmentation software.

References

1. Burgoyne CF, Downs JC, Bellezza AJ, Suh JK, Hart RT. The optic nerve head as a biomechanical structure: a new paradigm for understanding the role of IOP-related stress and strain in the pathophysiology of glaucomatous optic nerve head damage. *Prog Retin Eye Res*. 2005;24:39–73.

2. Sigal IA, Flanagan JG, Ethier CR. Factors influencing optic nerve head biomechanics. *Invest Ophthalmol Vis Sci*. 2005; 46:4189–4199.
3. Anderson DR, Hendrickson A. Effect of intraocular pressure on rapid axoplasmic transport in monkey optic nerve. *Invest Ophthalmol*. 1974;13:771–783.
4. Gaasterland D, Tanishima T, Kuwabara T. Axoplasmic flow during chronic experimental glaucoma. 1. Light and electron microscopic studies of the monkey optic nervehead during development of glaucomatous cupping. *Invest Ophthalmol Vis Sci*. 1978;17:838–846.
5. Minckler DS, Bunt AH, Johanson GW. Orthograde and retrograde axoplasmic transport during acute ocular hypertension in the monkey. *Invest Ophthalmol Vis Sci*. 1977;16: 426–441.
6. Morgan WH, Yu DY, Cooper RL, Alder VA, Cringle SJ, Constable IJ. The influence of cerebrospinal fluid pressure on the lamina cribrosa tissue pressure gradient. *Invest Ophthalmol Vis Sci*. 1995;36:1163–1172.
7. Burgoyne CF, Downs JC. Premise and prediction-how optic nerve head biomechanics underlies the susceptibility and clinical behavior of the aged optic nerve head. *J Glaucoma*. 2008;17:318–328.
8. Meirelles SH, Mathias CR, Bloise RR, et al. Evaluation of the factors associated with the reversal of the disc cupping after surgical treatment of childhood glaucoma. *J Glaucoma*. 2008; 17:470–473.
9. Wu SC, Huang SC, Kuo CL, Lin KK, Lin SM. Reversal of optic disc cupping after trabeculotomy in primary congenital glaucoma. *Can J Ophthalmol*. 2002;37:337–341.
10. Parrish RK II, Feuer WJ, Schiffman JC, Lichter PR, Musch DC. Five-year follow-up optic disc findings of the Collaborative Initial Glaucoma Treatment Study. *Am J Ophthalmol*. 2009; 147:717–724. e711.
11. Pederson JE, Herschler J. Reversal of glaucomatous cupping in adults. *Arch Ophthalmol*. 1982;100:426–431.
12. Figus M, Lazzeri S, Nardi M, Bartolomei MP, Ferreras A, Fogagnolo P. Short-term changes in the optic nerve head and visual field after trabeculectomy. *Eye (Lond)*. 2011;25:1057–1063.
13. Irak I, Zangwill L, Garden V, Shakiba S, Weinreb RN. Change in optic disk topography after trabeculectomy. *Am J Ophthalmol*. 1996;122:690–695.
14. Lesk MR, Spaeth GL, Azuara-Blanco A, et al. Reversal of optic disc cupping after glaucoma surgery analyzed with a scanning laser tomograph. *Ophthalmology*. 1999;106:1013–1018.
15. Paranhos A Jr, Lima MC, Salim S, Caprioli J, Shields MB. Trabeculectomy and optic nerve head topography. *Braz J Med Biol Res*. 2006;39:149–155.
16. Park KH, Kim DM, Youn DH. Short-term change of optic nerve head topography after trabeculectomy in adult glaucoma patients as measured by Heidelberg retina tomograph. *Korean J Ophthalmol*. 1997;11:1–6.
17. Topouzis F, Peng F, Kotas-Neumann R, et al. Longitudinal changes in optic disc topography of adult patients after trabeculectomy. *Ophthalmology*. 1999;106:1147–1151.
18. Bowd C, Weinreb RN, Lee B, Emdadi A, Zangwill LM. Optic disk topography after medical treatment to reduce intraocular pressure. *Am J Ophthalmol*. 2000;130:280–286.
19. Meredith SP, Swift L, Eke T, Broadway DC. The acute morphologic changes that occur at the optic nerve head induced by medical reduction of intraocular pressure. *J Glaucoma*. 2007;16:556–561.
20. van Velthoven ME, Faber DJ, Verbraak FD, van Leeuwen TG, de Smet MD. Recent developments in optical coherence tomography for imaging the retina. *Prog Retin Eye Res*. 2007;26:57–77.
21. Wojtkowski M, Srinivasan V, Fujimoto JG, et al. Three-dimensional retinal imaging with high-speed ultrahigh-resolution optical coherence tomography. *Ophthalmology*. 2005; 112:1734–1746.
22. Spaide RF, Koizumi H, Pozzoni MC. Enhanced depth imaging spectral-domain optical coherence tomography. *Am J Ophthalmol*. 2008;146:496–500.
23. Inoue R, Hangai M, Kotera Y, et al. Three-dimensional high-speed optical coherence tomography imaging of lamina cribrosa in glaucoma. *Ophthalmology*. 2009;116:214–222.
24. Lee EJ, Kim TW, Weinreb RN, Park KH, Kim SH, Kim DM. Visualization of the lamina cribrosa using enhanced depth imaging spectral-domain optical coherence tomography. *Am J Ophthalmol*. 2011;152:87–95. e81.
25. Park HY, Jeon SH, Park CK. Enhanced depth imaging detects lamina cribrosa thickness differences in normal tension glaucoma and primary open-angle glaucoma. *Ophthalmology*. 2012;119:10–20.
26. Park SC, De Moraes CG, Teng CC, Tello C, Liebmann JM, Ritch R. Enhanced depth imaging optical coherence tomography of deep optic nerve complex structures in glaucoma. *Ophthalmology*. 2012;119:3–9.
27. Agoumi Y, Sharpe GP, Hutchison DM, Nicolela MT, Artes PH, Chauhan BC. Laminar and prelaminar tissue displacement during intraocular pressure elevation in glaucoma patients and healthy controls. *Ophthalmology*. 2011;118:52–59.
28. Strouthidis NG, Yang H, Fortune B, Downs JC, Burgoyne CF. Detection of optic nerve head neural canal opening within histomorphometric and spectral domain optical coherence tomography data sets. *Invest Ophthalmol Vis Sci*. 2009;50: 214–223.
29. Strouthidis NG, Yang H, Reynaud JF, et al. Comparison of clinical and spectral domain optical coherence tomography optic disc margin anatomy. *Invest Ophthalmol Vis Sci*. 2009; 50:4709–4718.
30. Hayreh SS. Pathogenesis of cupping of the optic disc. *Br J Ophthalmol*. 1974;58:863–876.
31. Jonas JB, Berenshtein E, Holbach L. Anatomic relationship between lamina cribrosa, intraocular space, and cerebrospinal fluid space. *Invest Ophthalmol Vis Sci*. 2003;44:5189–5195.
32. Quigley HA, Hohman RM, Addicks EM, Massof RW, Green WR. Morphologic changes in the lamina cribrosa correlated with neural loss in open-angle glaucoma. *Am J Ophthalmol*. 1983; 95:673–691.
33. Levy NS, Crapps EE. Displacement of optic nerve head in response to short-term intraocular pressure elevation in human eyes. *Arch Ophthalmol*. 1984;102:782–786.
34. Trible JR, Sergott RC, Spaeth GL, et al. Trabeculectomy is associated with retrobulbar hemodynamic changes. A color Doppler analysis. *Ophthalmology*. 1994;101:340–351.
35. Minckler DS, Bunt AH. Axoplasmic transport in ocular hypotony and papilledema in the monkey. *Arch Ophthalmol*. 1977;95:1430–1436.
36. Kawasaki A, Purvin V. Unilateral optic disc edema following trabeculectomy. *J Neuroophthalmol*. 1998;18:121–123.
37. Nicolela MT, Soares AS, Carrillo MM, Chauhan BC, LeBlanc RP, Artes PH. Effect of moderate intraocular pressure changes on topographic measurements with confocal scanning laser tomography in patients with glaucoma. *Arch Ophthalmol*. 2006;124:633–640.
38. Morgan WH, Chauhan BC, Yu DY, Cringle SJ, Alder VA, House PH. Optic disc movement with variations in intraocular and cerebrospinal fluid pressure. *Invest Ophthalmol Vis Sci*. 2002; 43:3236–3242.
39. Strouthidis NG, Fortune B, Yang H, Sigal IA, Burgoyne CF. Effect of acute intraocular pressure elevation on the monkey optic nerve head as detected by spectral domain optical

coherence tomography. *Invest Ophthalmol Vis Sci*. 2011;52:9431–9437.

40. Yan DB, Coloma FM, Metheetrairut A, Trope GE, Heathcote JG, Ethier CR. Deformation of the lamina cribrosa by elevated intraocular pressure. *Br J Ophthalmol*. 1994;78:643–648.
41. Grytz R, Sigal IA, Ruberti JW, Meschke G, Downs JC. Lamina cribrosa thickening in early glaucoma predicted by a microstructure motivated growth and remodeling approach. *Mech Mater*. 2012;44:99–109.
42. Sigal IA, Ethier CR. Biomechanics of the optic nerve head. *Exp Eye Res*. 2009;88:799–807.
43. Sigal IA, Flanagan JG, Tertinegg I, Ethier CR. Predicted extension, compression and shearing of optic nerve head tissues. *Exp Eye Res*. 2007;85:312–322.
44. Sigal IA, Flanagan JG, Tertinegg I, Ethier CR. Modeling individual-specific human optic nerve head biomechanics. Part II: influence of material properties. *Biomech Model Mechanobiol*. 2009;8:99–109.
45. Jonas JB, Berenshtein E, Holbach L. Lamina cribrosa thickness and spatial relationships between intraocular space and cerebrospinal fluid space in highly myopic eyes. *Invest Ophthalmol Vis Sci*. 2004;45:2660–2665.
46. Sigal IA, Yang H, Roberts MD, et al. IOP-induced lamina cribrosa deformation and scleral canal expansion: independent or related? *Invest Ophthalmol Vis Sci*. 2011;52:9023–9032.
47. Sigal IA, Bilonick RA, Kagemann L, et al. The optic nerve head as a robust biomechanical system. *Invest Ophthalmol Vis Sci*. 2012;53:2658–2667.